Supporting Information

Rivera-Mulia et al. 10.1073/pnas.1711613114

SI Materials and Methods

Cell Culture. Primary cells were obtained from Coriell Institute for Medical Research, from the Progeria Research Foundation, and from donors from the CHRU Montpellier cohort (Table S1). Human primary fibroblasts were maintained in DMEM (Invitrogen) containing 10% heat-inactivated FBS (PAA), 2 mM L-glutamine, and 1% penicillin and streptomycin (Invitrogen). hESCs and iPSCs were maintained as feeder-free cultures on Matrigel (BD Biosciences) with chemically defined mTeSR medium (STEMCELL Technologies), as previously described (1).

Reprogramming into iPSCs. Primary fibroblasts were reprogrammed to iPSCs by infection with either lentiviral or Sendai viral vectors containing reprogramming factors: OCT4, SOX2, KLF4, and C-MYC. Vectors were obtained from Addgene (2). The 293T cell line (Invitrogen) was used to produce transgene-expressing lentiviruses. Human primary fibroblasts were incubated overnight with equal amounts of supernatants containing each virus. Six days after transduction, cells were harvested and replated on a feeder layer. The next day, the medium was replaced with hESC medium supplemented with 10 ng/mL basic fibroblast growth factor (bFGF). The medium was changed every other day. Thirty-four days after transduction, colonies were picked and transferred onto a feeder layer with 2 mL of hESC medium supplemented with 10 ng/mL bFGF in 35-mm dishes.

Redifferentiation of iPSCs. iPSCs were differentiated as previously described as embryoid bodies in AggreWell EB Formation Medium (STEMCELL Technologies) supplemented with 0.3 mM ascorbic acid (Sigma-Aldrich), 10 ng/mL TGFβ2 (R&D Systems), and ITS Supplement-A (Invitrogen). Embryoid bodies were attached to a gelatin-coated dish and were cultured for 10 d in DMEM (with high glucose) (Invitrogen) supplemented with ascorbic acid and 20% FBS. Cells that grew out from embryoid bodies were passaged and cultured every week to obtain consistent spindle-shaped cells.

Immunofluorescence. Cells were grown in coverslips, fixed with 4% paraformaldehyde, and permeabilized (PBS/0.5% Triton-X 100). Immunodetection was performed by 1-h incubation in blocking buffer (PBS/0.05% Tween-20, 5% BSA), followed by incubation with the primary antibodies mouse anti-H2AX (MA1-2022; Thermo Fisher) and goat anti-lamin B (sc-6217; Santa Cruz) for 1 h, two washes in PBS/0.5% Tween-20, 1 h of incubation with secondary antibodies (donkey anti-mouse Alexa-Fluor 488; donkey anti-mouse Alexa-Fluor 568; and donkey anti-goat Alexa-Fluor 647) (Invitrogen), and DNA was labeled by DAPI staining. Images were collected using a DeltaVision microscope (Applied Precision) equipped with a CoolSNAP HQ camera (Roper Scientific). 3D images were captured at different stage positions and were processed using deconvolution software (softWoRx 3.5.0; Applied Precision).

Genome-Wide RT Profiling. Genome-wide RT profiles were constructed as previously described (3, 4). Briefly, cells were pulse labeled with BrdU, separated into early and late S-phase fractions by flow cytometry, and processed by either Repli-ChIP or Repli-seq. For Repli-ChIP, BrdU-substituted DNA from early and late S-phase populations was immunoprecipitated, differentially labeled, and cohybridized to a whole-genome oligonucleotide microarray. Microarray hybridization and data extraction were performed according to standard NimbleGen procedures. For Repli-seq, sequencing libraries of BrdU-substituted DNA from early and late fractions were prepared by NEBNext Ultra DNA Library Prep Kit for Illumina (E7370; New England Biolabs). Sequencing was performed on an Illumina-HiSeq 2500 sequencing system by 50-bp single-end reads. Reads with quality scores above 30 were mapped to the Hg19 reference genome using bowtie2. Approximately 8 million uniquely mapped reads were obtained from each library. Read counts were binned into 5-kb nonoverlapping windows, and log2 ratios of read-counts between early and late fractions were calculated.

Clustering Analysis. RT profiles were expressed as numeric vectors. Nonoverlapping and variable regions (200-kb windows) were defined as those with differences ≥1 in pairwise comparisons between all samples (Fig. 2*A*). Unsupervised hierarchical and *k-means* clustering analysis were performed using Cluster 3.0 (5). Heatmaps and dendrograms were generated in Java TreeView (6). GO analysis was performed with the GREAT Tool (7). Branches of the dendrogram were constructed based on the correlation values (distance = 1 − correlation value).

qRT-PCR. Total RNA was extracted with RNeasy (Qiagen), according to the manufacturer's instructions. First-strand cDNA was synthesized with SuperScript III (Invitrogen). Isoform-specific primers were designed at exon junctions and optimized to have comparable efficiencies (Fig. S2*C*). All reactions were performed with FastStart SYBR Green Master (ROX) (Roche). qPCR reactions were tripled and performed in the ABI 7500 Fast system through 40 cycles (15 s at 95 °C, 45 s at 60 °C). CT values were generated by ABI software, and the relative gene expression was calculated by ΔΔCT method using *HPRT1* gene as reference.

1. Ludwig TE, et al. (2006) Feeder-independent culture of human embryonic stem cells. *Nat Methods* 3:637–646.
2. Yu J, et al. (2007) Induced pluripotent stem cell lines derived from human somatic cells. *Science* 318:1917–1920.
3. Ryba T, Battaglia D, Pope BD, Hiratani I, Gilbert DM (2011) Genome-scale analysis of replication timing: From bench to bioinformatics. *Nat Protoc* 6:870–895.
4. Marchal C, et al. (2017) Repli-seq: Genome-wide analysis of replication timing by next-generation sequencing. *Nat Protoc*, in press.
5. de Hoon MJL, Imoto S, Nolan J, Miyano S (2004) Open source clustering software. *Bioinformatics* 20:1453–1454.
6. Saldanha AJ (2004) Java Treeview–Extensible visualization of microarray data. *Bioinformatics* 20:3246–3248.
7. McLean CY, et al. (2010) GREAT improves functional interpretation of cis-regulatory regions. *Nat Biotechnol* 28:495–501.

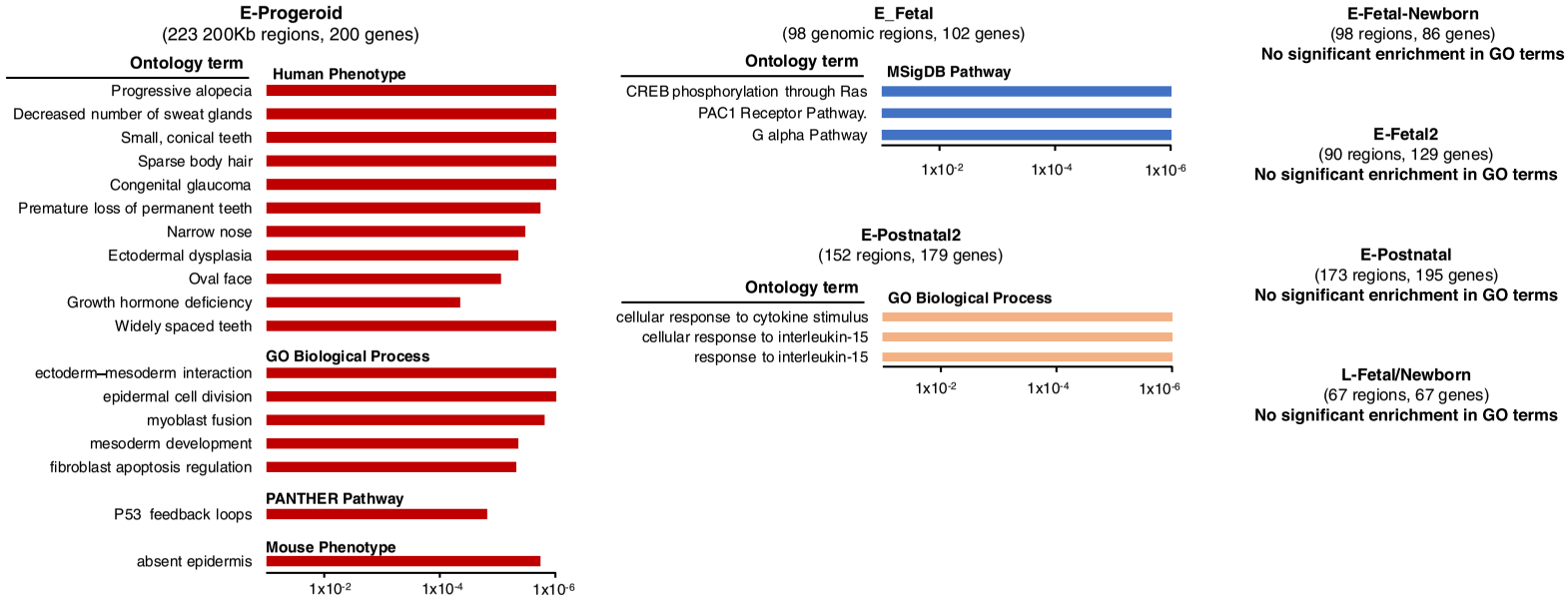

Fig. S1. Gene-expression analysis of HGPS and control samples. Ontology analysis enrichment for each of the RT signatures shown in Fig. 1*B*. Statistical significance measured by binomial test using the GREAT Tool (1). The number of 200-kb windows and genes per RT signature are shown.

1. Saldanha AJ (2004) Java Treeview–Extensible visualization of microarray data. *Bioinformatics* 20:3246–3248.

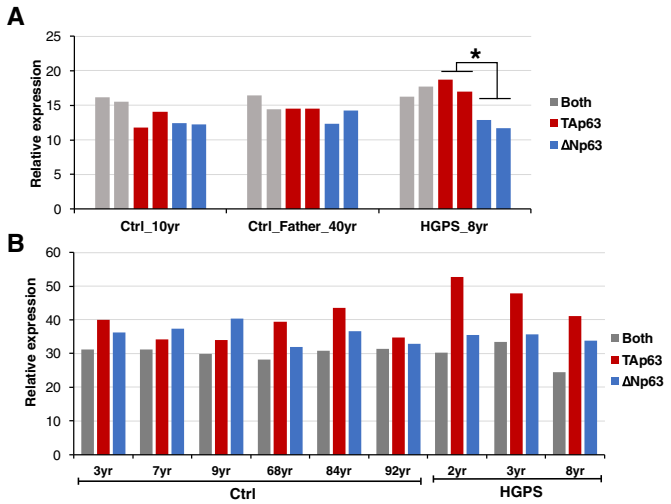

C

Amplicon	Primer	Sequence	Size	Slope	R2	Efficiency
TAp63	640	TGTATCCGCATGCAGGACT	127	-3.76	0.986	84.483
	641	CTGTGTTATAGGGACTGGTGGAC				
ΔNp63	654	GTCAGTTTCTTAGCGAGG	114	-3.11	0.955	109.668
	655	CAGACTTGCCAGATCATC				
Progerin	676	GGCTCAGGAGCCCAGAGC	84	-3.93	0.987	79.474
	677	GCAGGAAGCCTCCACCCC				
LaminA	678	GGGCGGACCCATCTCCTCT	98	-3.518	0.996	92.421
	679	TGTCCCCGAAGCTGCCAC				
HPRT1	670	CCTGGCGTCGTGATTAGTGAT	131	-3.67	0.988	87.016
	671	AGACGTTCAGTCCTGTCCATAA				

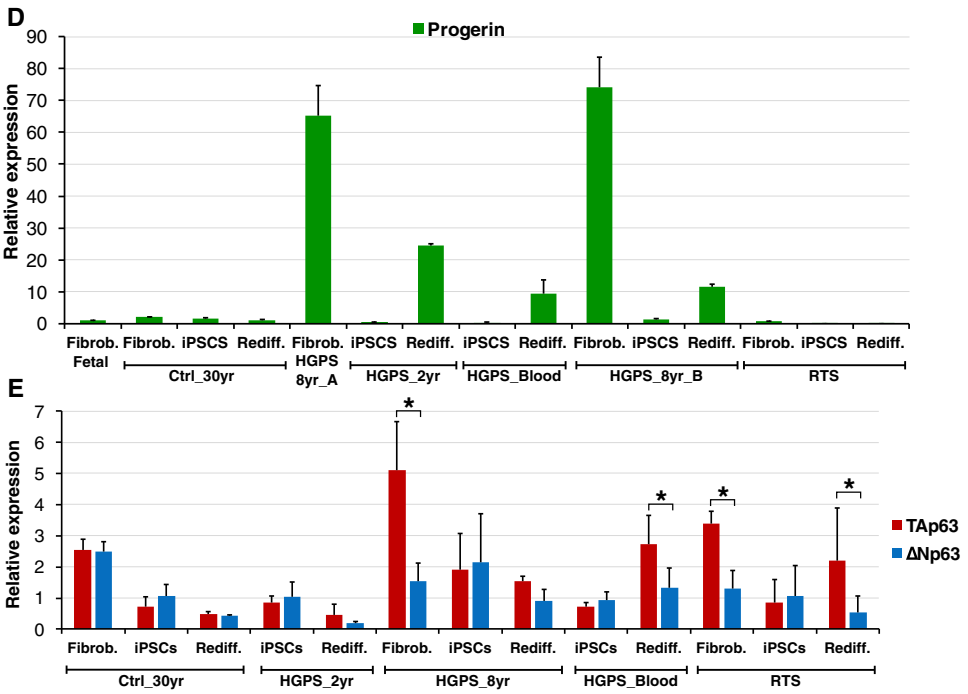

Fig. S2. Gene-expression analysis of HGPS and control samples. (*A* and *B*) A significant increase in TAp63 isoforms is observed in HGPS fibroblasts compared with healthy donors of distinct ages. Data were derived from array expression analysis of normal and HGPS cells by analyzing isoform-specific array probes against *TP63*. No significant differences were observed for probes that hybridize to both isoforms. Significant differences are shown (*$P < 0.05$). Data in *A* were obtained from ref. 1, and data in *B* were obtained from ref. 2. (*C*) Specific amplicons and oligo sequences designed for qRT-PCR analysis of the expression of *TP63* isoforms, progerin, and lamin A. (*D* and *E*) Relative quantification of progerin (*D*) and *TP63* isoforms (*E*) in samples derived from donors of distinct ages with progeroid syndromes and controls (age 0–96 y), iPSCs, and redifferentiated cells. Expression analysis was performed by qRT-PCR analysis with specific amplicons against TAp63 and ΔNp63 isoforms. Relative expression was normalized against the *HPRT1* gene as an endogenous control and fetal fibroblasts as a calibrator sample. Relative values were calculated by the ΔΔCT method (*$P < 0.05$).

1. McCord RP, et al. (2013) Correlated alterations in genome organization, histone methylation, and DNA-lamin A/C interactions in Hutchinson-Gilford progeria syndrome. *Genome Res* 23:260–269.
2. Kubben N, et al. (2016) Repression of the antioxidant NRF2 pathway in premature aging. *Cell* 165:1361–1374.

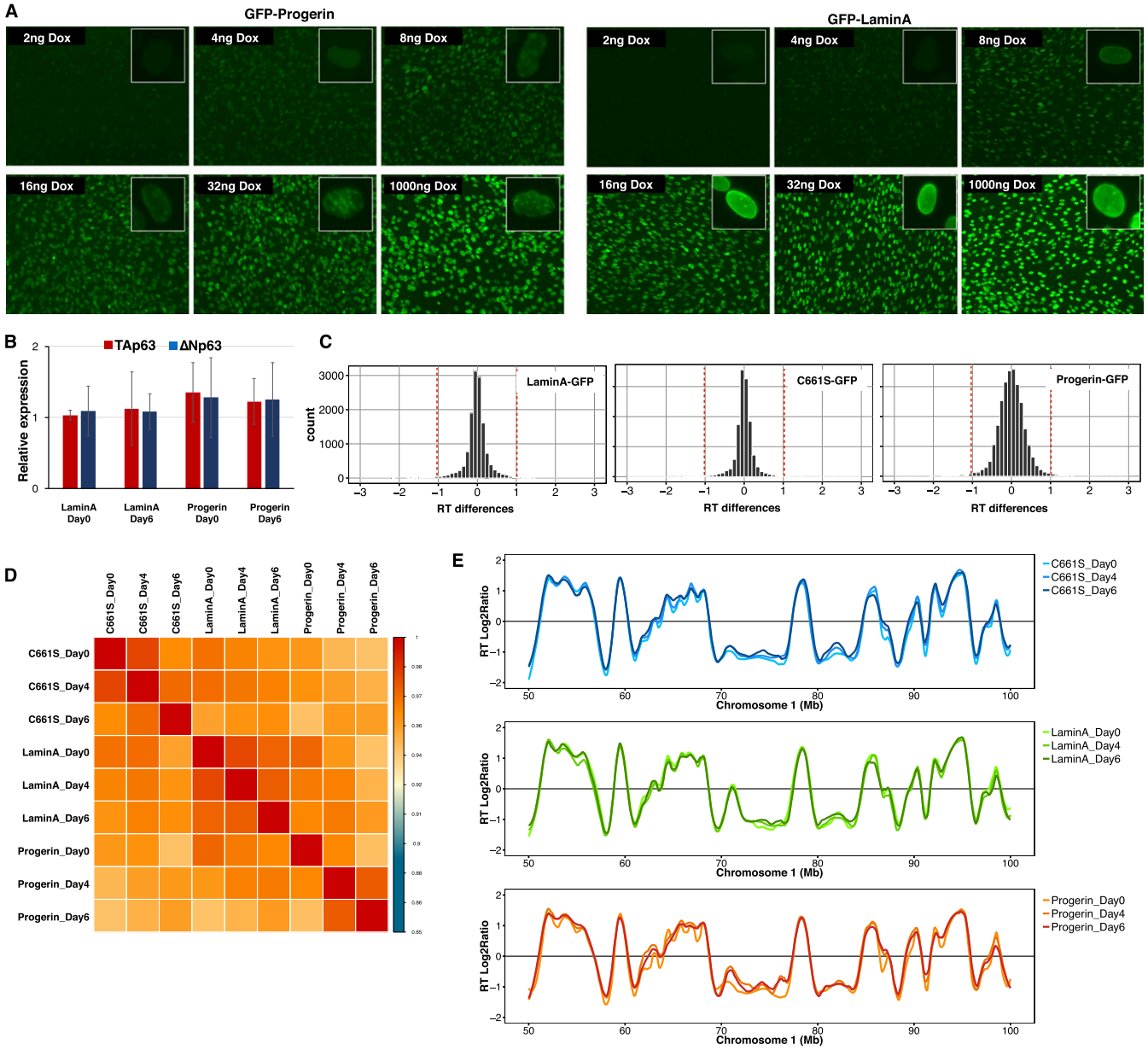

Fig. S3. Overexpression of progerin in normal fibroblasts recapitulates the nuclear alterations of HGPS. (*A*) Normal fibroblasts targeted with GFP-tagged lamin A or progerin or C661S (engineered farnesylation-defective progerin) vectors were induced with distinct concentrations of doxycycline (DOX). The optimal concentration of doxycycline DOX was determined to induce comparable levels of GFP fluorescence. (Magnification: 10×; *Insets*, 40×.) (*B*) Relative expression levels of TAp63 and ΔNp63 after overexpression of lamin A-GFP or progerin-GFP. (*C*) RT differences after induction of lamin A-GFP, C661S-GFP, or progerin-GFP for 6 d. (*D*) Genome-wide correlation matrix of RT programs of fibroblasts at distinct days after induction of lamin A-GFP, C661S-GFP, or progerin-GFP. (*E*) RT profiles of an exemplary genomic region at chromosome 1 show identical RT after induction of lamin A-GFP, C661S-GFP, or progerin-GFP.

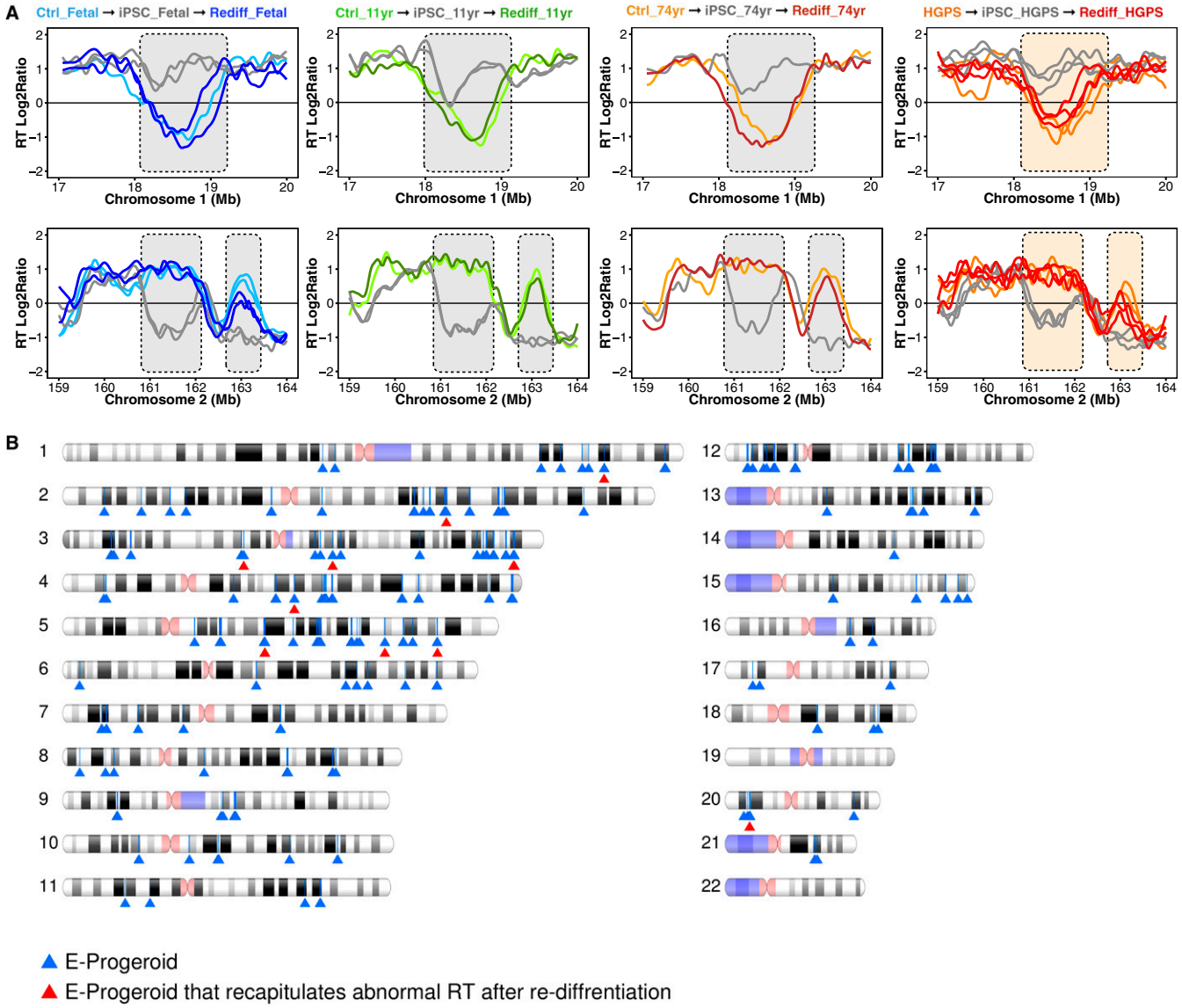

Fig. S4. The RT program is fully reset to pluripotency after reprogramming to iPSCs and is reestablished upon redifferentiation. (*A*) RT profiles of exemplary genomic regions show the dynamic changes in RT after reprogramming and redifferentiation of cells from healthy donors of distinct ages and fibroblasts derived from HGPS patients. (*B*) Chromosome location of the genomic regions that replicate early in progeroid diseases. From 223 genomic regions (each 200 kb) identified within the RT signature E-progeroid, only 10 reacquired the progeroid-specific abnormal RT pattern upon redifferentiation of patient-derived iPSCs; these included the locus of *TP63*.

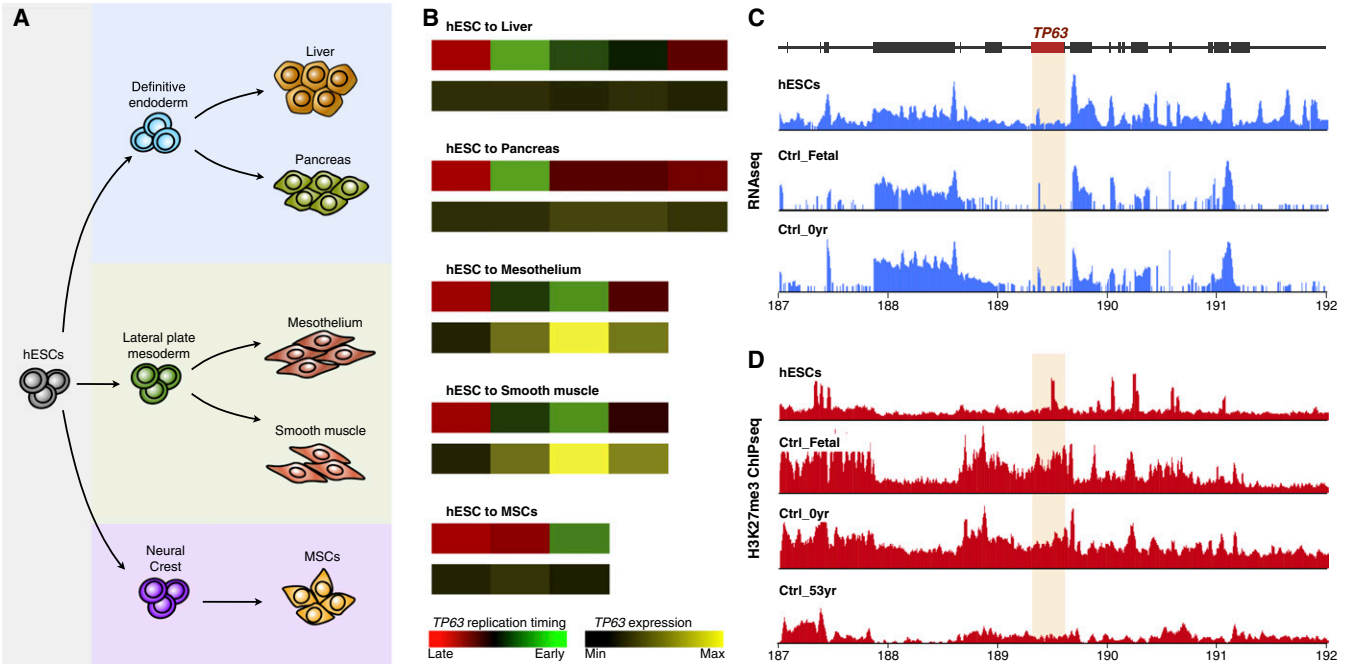

Fig. S5. Dynamic changes of the *TP63* locus during normal cell-fate commitment. (*A*) Schematic depiction of distinct cell types representing intermediate stages of hESC differentiation toward endoderm, mesoderm, ectoderm, and neural crest (NC). MSCs, mesenchymal stem cells. (*B*) The *TP63* gene changes to early replication during the first stages of development and switches back to late replication in later stages in all differentiation pathways toward cell types representing all three germ layers. Expression levels show that *TP63* is highly induced only when the gene is replicated early during S-phase. (*C*) Decreasing expression of *TP63* is observed from hESCs to fetal and newborn stages in fibroblasts from healthy donors. (*D*) *TP63* is enriched in H3K27me3 in normal fetal/postnatal fibroblasts but is depleted in fibroblasts from old donors.

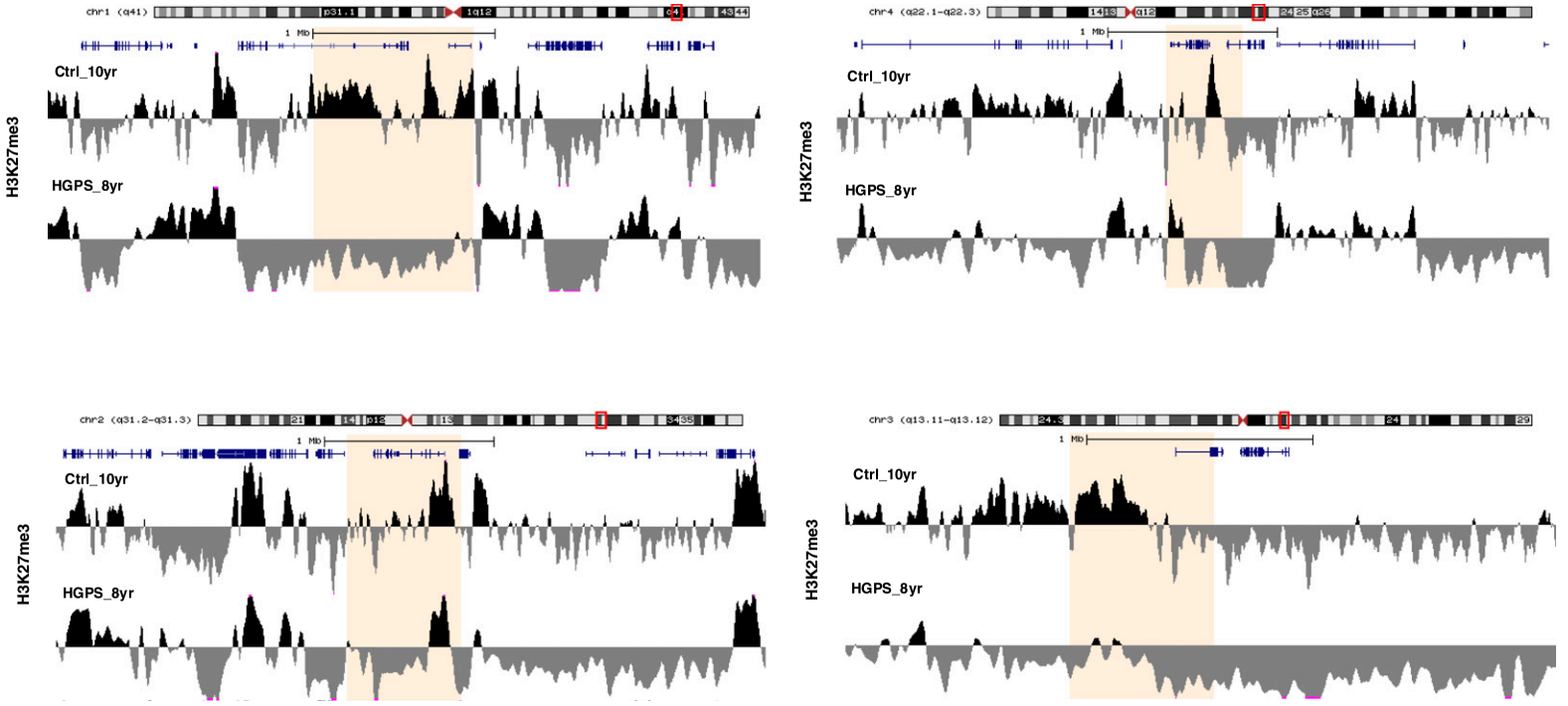

Fig. S6. Loss of H3K27me3 at the genomic regions from the progeroid-specific RT signature. H3K27me3 data from a progeroid patient (cell line HGADFN167 = HGPS_8yr) and from a healthy donor of similar age are shown for exemplary regions from the progeroid-specific RT signature. H3K27me3 datasets were obtained from ref. 1.

1. McCord RP, et al. (2013) Correlated alterations in genome organization, histone methylation, and DNA-lamin A/C interactions in Hutchinson-Gilford progeria syndrome. *Genome Res* 23:260–269.

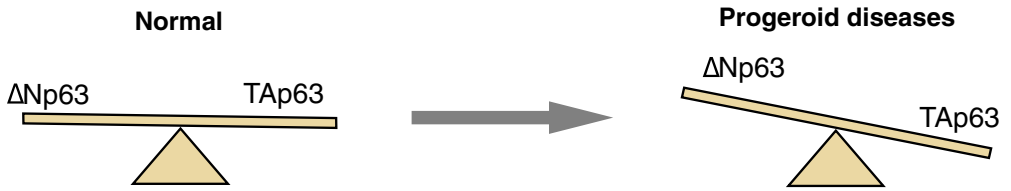

Development	
Proper ectodermal morphogenesis	Altered ectodermal differentiation
Normal epithelial and gland development	Epithelial and gland development defects
Proper limb morphogenesis	limb malformations
Epidermis	
Epidermal stem cells renewal	Epidermal stem cells depletion
High regenerative potential	Impaired regenerative potential
High proliferative capacity	Increased cellular senescence
Proper DNA repair	Increased activation of apoptosis
Proper terminal epidermal differentiation	Impaired DNA repair

Fig. S7. Model of *TP63* alterations in progeroid diseases. Altered expression of *TP63* isoforms is associated with distinct defects in ectodermal development and epidermis regulation.

Table S1. Summary of samples analyzed

Cell type/ sample no.	Sample ID	Sample name	Group	Age, y	Gender	RT method	Source	Mutation	GEO
Fibroblasts									
1	AG11513	HGPS_8yr_A	HGPS	8	Female	Repli-ChIP	Skin (leg)	*LMNA*	GSE98471
2	HGADFN003	HGPS_2yr	HGPS	2	Male	Repli-seq	Skin (foreskin)	*LMNA*	GSE98472
3	HGADFN167	HGPS_8yr_B	HGPS	8	Male	Repli-seq	Skin (arm)	*LMNA*	GSE98472
4	AG17524	RTS_4yr	RTS	4	Female	Repli-seq	Skin	*RECQL4*	GSE98472
5	AG05013	RTS_10yr	RTS	10	Male	Repli-seq	Skin	*RECQL4*	GSE98472
6	RTS_43	RTS_43yr	RTS	43	Female	Repli-seq	Skin	*RECQL4*	GSE98472
7	IMR90	Ctrl_Fetal	Fetal	0	Female	Repli-ChIP	Lung	-	GSE38460
8	PreS_IMR90	PreS_Fetal	Fetal	0	Female	Repli-ChIP	Lung	-	GSE98471
9	IMR90_RIS	OIS_Fetal	Fetal	0	Female	Repli-ChIP	Lung	-	GSE38460
10	BJ	Ctrl_0yr	Newborn	0	Male	Repli-ChIP	Skin (foreskin)	-	GSE98471
11	PreS_BJ	PreS_0yr	Newborn	0	Male	Repli-seq	Skin (foreskin)	-	GSE98472
12	GM03348	Ctrl_10yr	Young	10	Male	Repli-seq	Skin	-	GSE98472
13	GM01864	Ctrl_11yr	Young	11	Male	Repli-seq	NS	-	GSE98472
14	Fibro_74yr	Ctrl_74yr	Aged	74	Male	Repli-ChIP	Skin	-	GSE98471
15	PreS_Fibro74yr	PreS_74yr	Aged	74	Male	Repli-ChIP	Skin	-	GSE98471
16	GM04204	Ctrl_81yr	Aged	81	Male	Repli-seq	NS	-	GSE98472
17	GM01706	Ctrl_82yr	Aged	82	Female	Repli-seq	Skin (arm)	-	GSE98472
18	AG04064	Ctrl_92yr	Aged	92	Male	Repli-seq	Skin (arm)	-	GSE98472
19	AG04059	Ctrl_96yr	Aged	96	Male	Repli-ChIP	Skin (arm)	-	GSE98471
iPSC									
20	iPSC_HGADFN003	iPSC_HGPS_2yr	HGPS	2	Male	Repli-seq	Skin (foreskin)	*LMNA*	GSE98472
21	iPSC_HGADFN167	iPSC_HGPS_8yr	HGPS	8	Male	Repli-seq	Skin (arm)	*LMNA*	GSE98472
22	iPSC_Prog_Blood	iPSC_HGPS_Blood	HGPS	NS	Male	Repli-seq	Blood (PBMC)	*LMNA*	GSE98472
23	iPSC_RTS	iPSC_RTS	RTS	43	Female	Repli-seq	Skin	*RECQL4*	GSE98472
24	iPSC_IMR90_R1	iPSC_Fetal_R1	Fetal	0	Female	Repli-ChIP	Lung	-	GSE98471
25	iPSC_IMR90_R2	iPSC_Fetal_R2	Fetal	0	Female	Repli-seq	Lung	-	GSE98472
26	iPSC_BJ	iPSC_0yr	Newborn	0	Male	Repli-seq	Skin (foreskin)	-	GSE98472
27	iPSC_GM01864_A	iPSC_11yr	Young	11	Male	Repli-seq	NS	-	GSE98472
28	iPSC_GM01864_B	iPSC_11yr	Young	11	Male	Repli-seq	NS	-	GSE98472
29	iPS4_R1	iPS4_30yr	Adult	30	Male	Repli-seq	Skin	-	GSE20027
30	iPS5_R1	iPS5_30yr	Adult	30	Male	Repli-seq	Skin	-	GSE20027
31	iPSC_HGMDFN090	iPSC_M_30yr	Adult	30	Female	Repli-seq	Skin	-	GSE98472
32	iPSC_Fibro74yr	iPSC_74yr	Aged	74	Male	Repli-ChIP	Skin	-	GSE98471
33	iPSC_GM01706_A	iPSC_82yr	Aged	82	Female	Repli-seq	Skin (arm)	-	GSE98472
34	iPSC_GM01706_B	iPSC_82yr	Aged	82	Female	Repli-seq	Skin (arm)	-	GSE98472
35	iPSC_AG04064	iPSC_92yr	Aged	92	Male	Repli-ChIP	Skin (arm)	-	GSE98471
ESC (control)									
36	ESC_BG01	ESC_BG01	ESC	0	Male	Repli-ChIP	Blastocysts	-	GSE20027
37	ESC_BG02	ESC_BG02	ESC	0	Male	Repli-ChIP	Blastocysts	-	GSE20027
38	ESC_H1	ESC_H1	ESC	0	Male	Repli-ChIP	Blastocysts	-	GSE63428
39	ESC_H7	ESC_H7	ESC	0	Female	Repli-ChIP	Blastocysts	-	GSE20027
40	ESC_H9	ESC_H9	ESC	0	Female	Repli-ChIP	Blastocysts	-	GSE98471
Redifferentiated									
41	Fibro_iPSC_HGADFN003	Redif_HGPS_2yrs	HGPS	2	Male	Repli-seq	Skin (foreskin)	*LMNA*	GSE98472
42	Fibro_iPSC_HGADFN167	Redif_HGPS_8yrs	HGPS	8	Male	Repli-seq	Skin (arm)	*LMNA*	GSE98472

Table S1. Cont.

Cell type/ sample no.	Sample ID	Sample name	Group	Age, y	Gender	RT method	Source	Mutation	GEO
43	Fibro_Prog_Blood	Redif_HGPS_Blood	HGPS	NS	Male	Repli-seq	Blood (PBMC)	*LMNA*	GSE98472
44	Fibro_iPSC_RTS	Redif_RTS	RTS	43	Female	Repli-seq	Skin	*RECQL4*	GSE98472
45	Fibro_H9	Redif_H9	Fetal	0	Female	Repli-ChIP	Blastocysts	-	GSE98471
46	Fibro_iPSC_IMR90	Redif_Fetal_R1	Fetal	0	Female	Repli-ChIP	Lung	-	GSE98471
47	Fibro_iPSC_IMR90	Redif_Fetal_R2	Fetal	0	Female	Repli-ChIP	Lung	-	GSE98471
48	Fibro_iPSC_Fibro_11yr	Redif_11yr	Young	11	Male	Repli-seq	NS	-	GSE98472
49	Fibro_iPSC_HGMDFN090	Redif_M_30yr	Adult	30	Female	Repli-seq	Skin	-	GSE98472
50	Fibro_iPSC_Fibro74yr	Redif_74yr	Aged	74	Male	Repli-ChIP	skin	-	GSE98471
52	Fibro_iPS_Fibro92yr	Redif_92yr	Aged	92	Male	Repli-ChIP	skin (arm)	-	GSE98471
Overexpression in WT cells									
53	Progerin_D0	Progerin_D0	Progerin overexpression	NS	NS	Repli-seq	Skin	-	GSE98472
54	Progerin_D4	Progerin_D4	Progerin overexpression	NS	NS	Repli-seq	Skin	-	GSE98472
55	Progerin_D6	Progerin_D6	Progerin overexpression	NS	NS	Repli-seq	Skin	-	GSE98472
56	LaminA_D0	LaminA_D0	LaminA overexpression	NS	NS	Repli-seq	Skin	-	GSE98472
57	LaminA_D4	LaminA_D4	LaminA overexpression	NS	NS	Repli-seq	Skin	-	GSE98472
58	LaminA_D6	LaminA_D6	LaminA overexpression	NS	NS	Repli-seq	Skin	-	GSE98472
59	C661S_D0	C661S_D0	C661S overexpression	NS	NS	Repli-seq	Skin	-	GSE98472
60	C661S_D4	C661S_D4	C661S overexpression	NS	NS	Repli-seq	Skin	-	GSE98472
61	C661S_D6	C661S_D6	C661S overexpression	NS	NS	Repli-seq	Skin	-	GSE98472

NS, not specified; PBMC, peripheral blood mononuclear cell.

Other Supporting Information Files

Dataset S1 (XLSX)